

# Remote performance check and automated failure identification for grid-connected PV systems – results and experiences from the test phase within the PVSAT-2 project

A. Drews<sup>1\*</sup>, E. Lorenz<sup>1</sup>, J. Betcke<sup>1</sup>, A.C. de Keizer<sup>2</sup>, W.G.J.H.M. van Sark<sup>2</sup>, H.G. Beyer<sup>3</sup>,  
W. Heydenreich<sup>4</sup>, E. Wiemken<sup>4</sup>, S. Stettler<sup>5</sup>, P. Toggweiler<sup>5</sup>, S. Bofinger<sup>6</sup>, M. Schneider<sup>6</sup>,  
G. Heilscher<sup>6</sup>, D. Heinemann<sup>1</sup>

<sup>1</sup> Oldenburg University, Dept. of Physics, Postfach 2503, 26111 Oldenburg; Germany

<sup>2</sup> Utrecht University, Copernicus Institute, Dept. of Science, Technology, and Society,  
Heidelberglaan 2, 3584 CH Utrecht, The Netherlands

<sup>3</sup> University of Applied Sciences Magdeburg-Stendal (FH), Institute of Electrical Engineering,  
Breidscheidstr. 2, 39114 Magdeburg, Germany

<sup>4</sup> Fraunhofer Institute for Solar Energy Systems, Heidenhofstr. 2, 79110 Freiburg, Germany

<sup>5</sup> Enecolo AG, Lindhofstr. 52, 8617 Moenchaltorf, Switzerland

<sup>6</sup> Meteocontrol GmbH, Spicherer Str. 48, 86157 Augsburg, Germany

\* Corresponding author, email: anja.drews@uni-oldenburg.de

## Abstract

Failure-free operation of grid-connected photovoltaic systems is important for the economic success of a system. Within the EU-funded project PVSAT-2, a service, based on satellite-derived irradiance data that detects automatically occurred system malfunctions, has been developed to ensure reliable operation of small systems up to 5 kW<sub>p</sub>.

The detection and identification of a failure is strongly influenced by the accuracy of the satellite-derived irradiance data. This accuracy changes with the predominant weather situation, e.g. under clear sky conditions the errors are low, while they increase under cloudy skies. This determines the quality of the PV simulation and finally the period of time that is needed to detect a failure. Under clear-sky conditions and high power production also a small failure (~15% energy loss) can be detected and identified within a few days. During winter time the energy loss has to be larger than 30% to be detected.

Keywords: performance check, automated failure detection, satellite data, PVSAT-2

## 1. Introduction

Failure-free operation of grid-connected photovoltaic (PV) systems, granting economic success, can be obtained only by regular performance checks. Especially small systems up to 5 kW<sub>p</sub> are often not monitored because additional hardware such as radiation sensors, data loggers, or other monitoring devices is required. This can be expensive and needs intensive maintenance. Furthermore, system faults or decreasing performance can stay unrecognised due to fluctuating energy yields caused by the highly variable solar resource if operators are no PV specialists.

Therefore, to secure the economical benefit for small systems especially in countries with a granted feed-in tariff, within the PVSAT-2 project a low-cost and easy-to-use service has been developed to assure maximum energy yields and to optimise system maintenance. The system's performance is checked on a daily basis by comparing the actual energy yield against an expected, simulated value. A PV simulation model, which employs inexpensive satellite-derived irradiance data instead of on-site measurements, calculates the expected energy yield. A local data logger, the only hardware on-site that is connected directly to the PV system, records the actual energy yield. It transmits the data every night to a central server. There, a failure detection routine checks automatically the performance of the system. In case of a detected malfunction, the most likely failure source is determined and the operator informed.

This contribution will give a short overview on the components of the PVSAT-2 routine. We will show selected results from major parts of the developed procedure.

Since the irradiation calculation dominates the quality of the whole procedure, results using

different satellite-derived irradiance data sets with different temporal and spatial resolution, are shown. The focus is set on the resulting quality of the PV simulation on the basis of selected PV systems where additional information such as irradiation measurements on the tilted plane are available. Experiences with the capabilities of the automated failure detection as obtained from a 10-month field test with 100 systems in Germany, Switzerland, and the Netherlands are summarised in the last part. More detailed information, especially on the single components of the PVSAT-2 scheme, can be found at [1].

## 2. The PVSAT-2 procedure

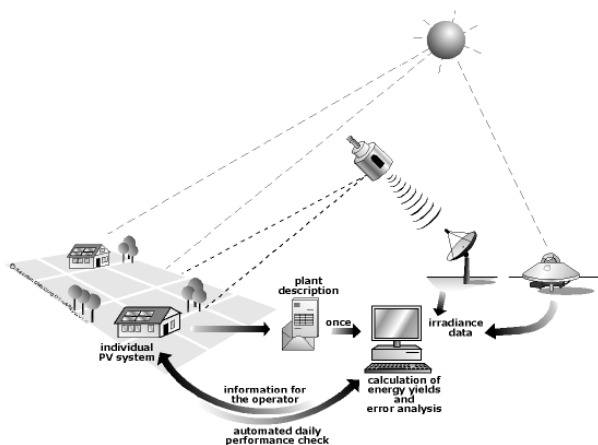


Fig. 1 PVSAT-2 scheme

The developed procedure as shown in Fig. 1 can shortly be described as follows: The actual energy yield of a PV system is recorded in 15-minute intervals and transmitted daily to a central server. To calculate the comparison value, global irradiance information is derived hourly by the Heliosat-method [2][3] from data of the geostationary Meteosat satellites. Its accuracy can be improved with ground measurements for certain meteorological situations by the method 'kriging-of-differences' [4][1]. The irradiance data from the selected site and the technical information on the system provide the main input for the PV simulation model which

calculates the expected energy yield of the system. The model accounts for crystalline silicon and the various thin film technologies [1]. The simulated energy yield is compared daily to the actual yield of the PV system. If the difference between the values exceeds a maximum of assumed uncertainty, the occurrence of a failure is detected. Then, two failure detection algorithms investigate the characteristics of the energy loss to identify the most likely failure source. The so-called 'footprint algorithm' focuses on the detection of shading, inverter malfunctions, and constant energy losses like string failures. It examines the dependence of the energy yield on the parameters time, normalised power production, and sun elevation using a special statistical approach of averaging, which reduces simulation errors from the uncertainties of the irradiance calculation. A failure pattern is extracted and compared to predefined failure pattern from a database. The second approach, the failure profiling, investigates the properties of the daily energy loss such as amount, duration, changes, correlation with neighbouring systems, and ambient temperature from the nearest weather station. It creates a failure profile by listing the attributes of the loss. These attributes are compared to known failure profiles. Excluding unlikely faults and narrowing down to the most probable failures determine the most likely failure sources. At last, the results of both routines are combined to a probability measure. 14 different failures can be detected (see Sec. 3.4, Tab.4). Finally, the operator of the system is informed about the system's performance.

## 3. Selected results

### 3.1 Data sets of satellite-derived irradiance and ground measurements

Three different irradiance data sets from the year 2005 have been evaluated for the use in the PVSAT-2 procedure: Meteosat-7, Meteosat-8, and Meteosat-8 refined with ground measurements. In 2004 and 2005 the two geostationary, meteorological satellites, Meteosat-7 and Meteosat-8 (MSG-1), have been in service in parallel. Meteosat-7, in operation since 1998, acquires images of Europe and Africa every 30 minutes in the visible part of the solar spectrum. Its spatial resolution is 5x7 km in Central Europe. Meteosat-8, a satellite of a new generation,

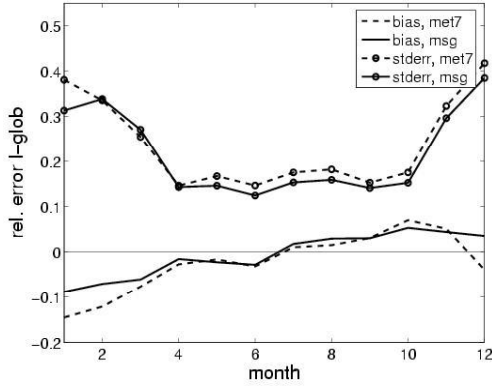


Fig. 2 Hourly accuracy of global irradiance as derived from Meteosat-7 and Meteosat-8 (MSG-1) data.

given standard error (stderr) is defined as the standard deviation of the error. Due to the higher temporal and spatial resolution of Meteosat-8 the standard error of 17.8% is lower than for Meteosat-7 (19.4%). Meteosat-7 underestimates the ground measurements with  $-1.7\%$  while Meteosat-8 has a lower bias of  $-0.6\%$ .

### 3.2 Accuracy of the PV simulation

Based on satellite-derived global irradiance data the expected output of the PV system is calculated. In a first step the global horizontal irradiance is converted to the module plane. In a second step a PV simulation model is applied. A detailed description can be found at [1].

The accuracy of the simulated PV system output based on Meteosat-7 data has been evaluated during the 10-month test phase (see [1]). Here, different data sets, as described in the preceding section, are compared against each other for their use in the PVSAT-2 procedure. Irradiance on the module plane and PV simulation is evaluated for calculations based on Meteosat-7, Meteosat-8 and for Meteosat-8 combined with ground measured irradiance. The comparison was done for three well-monitored example systems located in Southern Germany, orientated to the south with tilt angles between  $18^\circ$  and  $30^\circ$  for the year 2005. The irradiance on the module plane was measured using reference cells. Tab. 1 – Tab. 3 give the results for the irradiance on the module plane and for PV system power output for the different PV systems. Bias and standard error are provided on different time scales.

	$G_{\text{tilt, Met-7}}$	$G_{\text{tilt, Met-8}}$	$G_{\text{tilt, Met-8, kr}}$	$P_{\text{ac, Met-7}}$	$P_{\text{ac, Met-8}}$	$P_{\text{ac, Met-8, kr}}$
bias	2.3%	3.1	<b>1.7%</b>	2.3%	3.4%	<b>1.8%</b>
stderr, hourly	23.2%	23.2	<b>22.0%</b>	24.9%	25.9%	<b>24.0%</b>
stderr, daily	15.0%	14.0	<b>12.9%</b>	16.0%	16.0 %	<b>14.1%</b>
stderr, monthly	7.5%	4.3	<b>4.6%</b>	7.6%	5.0 %	<b>4.0%</b>

Tab. 1 Accuracy of the irradiance and the simulated power output on the tilted plane for system 1. kr: satellite data combined with ground measurements.

	$G_{\text{tilt, Met-7}}$	$G_{\text{tilt, Met-8}}$	$G_{\text{tilt, Met-8, kr}}$	$P_{\text{ac, Met-7}}$	$P_{\text{ac, Met-8}}$	$P_{\text{ac, Met-8, kr}}$
bias	2.9%	4.4 %	<b>1.5%</b>	-3.7%	<b>-2.1%</b>	-4.9%
stderr, hourly	24.1 %	24.0 %	<b>19.7%</b>	24.3%	24.8 %	<b>20.3%</b>
stderr, daily	15.0 %	14.3 %	<b>10.4%</b>	16.2%	17.1%	<b>12.7%</b>
stderr, monthly	5.9%	3.3%	<b>1.7%</b>	7.4 %	6.3%	<b>5.9 %</b>

Tab. 2 Accuracy of the irradiance and the simulated power output on the tilted plane for system 2. kr: satellite data combined with ground measurements.

operating since the beginning of 2004, provides a better temporal resolution of 15 minutes as well as a better spatial resolution of  $1.25 \times 1.75$  km in the high resolution visible channel (HRV). For a further improvement in accuracy, the Meteosat-8 data have been refined with ground measurements by the method 'kriging-of-differences'. Especially under conditions of low irradiance the improvements are significant [4].

To derive global irradiance from satellite data on the horizontal plane, an enhanced version of the Heliosat-method [3] has been applied. An accuracy assessment for the year 2005 and for 20 meteorological stations of the German Weather Service for hourly, daily, and monthly irradiance data has been performed. Fig. 2 shows the quality of hourly values over the year. The

	$G_{\text{tilt}}$ , Met-7	$G_{\text{tilt}}$ , Met-8	$G_{\text{tilt}}$ , <b>Met-8, kr</b>	$P_{\text{ac}}$ , Met-7	$P_{\text{ac}}$ , Met-8	$P_{\text{ac}}$ , <b>Met-8, kr</b>
bias	5.0%	<b>4.0 %</b>	5.0 %	0.4 %	-0.5%	<b>0.4 %</b>
stderr, hourly	23.7 %	<b>22.7 %</b>	22.8 %	23.6 %	<b>23.0 %</b>	23.1%
stderr, daily	12.5 %	11.1 %	<b>10.5%</b>	14.0%	13.0%	<b>12.7%</b>
stderr, monthly	7.2%	<b>2.9%</b>	3.6 %	6.8%	4.0%	<b>3.8 %</b>

Tab. 3 Accuracy of the irradiance and the simulated power output on the tilted plane for system 3. kr: satellite data combined with ground measurements.

The tables show:

- The application of kriging-of-differences leads to the best results, especially for system 2 a large improvement is achieved.
- The results for Meteosat-8 are slightly better than for Meteosat-7.
- The standard deviation of errors of the PV simulation is dominated by the standard deviation of the errors of the satellite-derived irradiance on the module plane. The bias for the irradiance on the module plane may differ from the bias of the PV simulation up to 5 %. This may be due to the choice of PV system parameters or to the accuracy of reference cells.
- The accuracy is increasing with increasing averaging period; the quality of monthly mean values is comparable to simulation results based on ground-measured irradiance.

The standard error and the bias of hourly values of the irradiance on the module plane are displayed over the month in Fig. 3. for the three different data sets. It illustrates that during summertime the best results are achieved with Meteosat-8 (MSG-1) due to the enhanced temporal

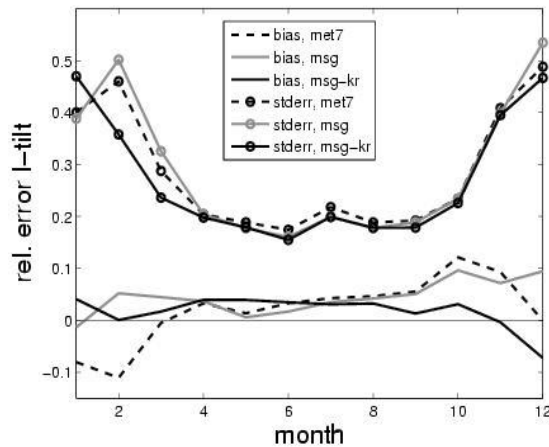


Fig. 3 Accuracy of hourly irradiance on array plane derived from Meteosat-7, Meteosat-8 data, and for Meteosat-8 data refined by kriging-of-differences. Evaluation for 3 PV systems.

and spatial resolution compared to Meteosat-7. There is no additional improvement by kriging-of-differences. During the winter period irradiance calculation only with satellite data is difficult, especially in the presence of snow. Here, interpolation with ground data leads to significantly better results.

### 3.3 Accuracy information for the failure detection routine

The calculated power output is provided with error margins in order to decide whether the difference between measured and simulated values is due to the uncertainty of irradiance data or due to a significant energy loss. This is illustrated in Fig. 4, where measured and simulated power output with error margins are displayed for two example days in June for system 1 for a Meteosat-8 based calculation. Fig. 4 shows the high quality of PV simulation for clear sky days with high power production, while

for cloudy days, especially for broken cloud situations, larger deviations between measured and simulated values are found. In order to account for this behaviour, error margins in dependence on the weather situation and the sun elevation where derived. The error margins denote maximum expected errors of simulation and are defined as two times the situation specific standard error.

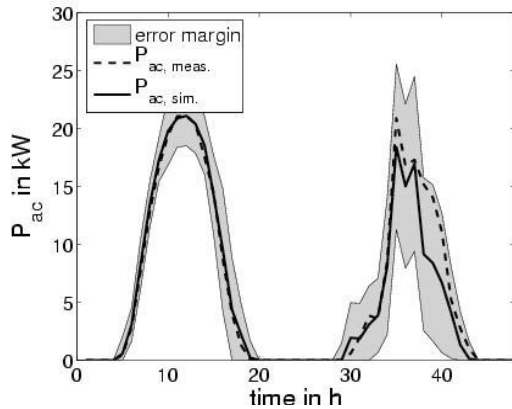


Fig. 4 Measured and simulated PV system power output with error margins of PV simulation.

found, when weather specific error margins are used. When using constant error margins the potential of high quality PV simulation for clear sky days cannot be used. Hourly values are necessary for the identification of reasons of system malfunction (extraction of typical error patterns by the footprint method).

- For daily values (middle figure) error margins are decreasing. On nice days the detection of system faults with an energy loss of ~15% is possible. During winter time, when the energy production is low, system faults may hardly be detected on a daily base.
- Using monthly values (right figure) error margins are below 30 %, also during wintertime. Hence system faults leading to major energy losses may be detected all over the year. During summer month also minor energy losses of 15 % can reliably be detected.

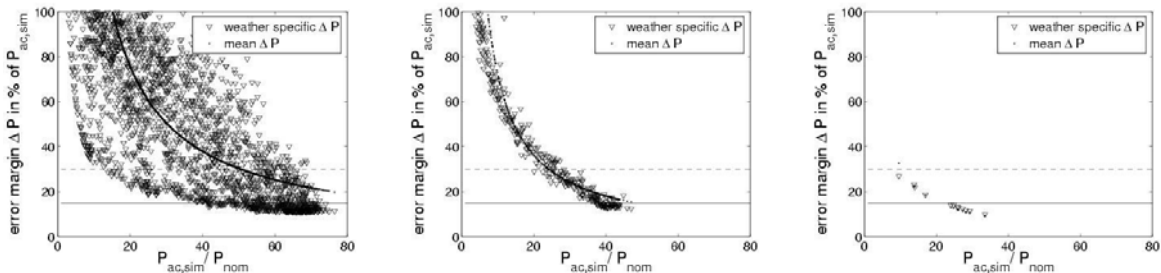


Fig. 5 Detectability of system failures in dependence of assumed simulation uncertainties on the considered time scales. left: hourly; mid: daily, right: monthly

The failure detection routine evaluates the energy yields on all time scales. This allows for fast failure detection on nice days with high power production. For less favourable conditions averaging as done in the footprint method reduces the uncertainty of simulation.

### 3.4 Capability of the failure detection routines

The functioning of the failure detection routines has been tested in the above mentioned field test. Constant feedback from the test users have shown the capabilities as well as improvement opportunities and limits. Tab. 2 lists the detectable failures.

Both failure detection methods, failure profiling and footprint, have been evaluated separately due to their different approaches. In the following the detection of shading is described for both approaches and concluding results for other failure types are given.

In the footprint method, shading is considered as time of day and sun elevation dependent shading. The sun elevation dependent shading is defined as an error at sun elevations lower than 20°. The time dependent shading is defined as an error early in the morning and late in the

In Fig. 5 the error margins for hourly, daily and monthly values are displayed over normalised energy production for system 1 for Meteosat-7 for a whole year. Situation specific error margins (weather specific  $\Delta P$ ) are compared to error margins assuming constant errors for all situations (mean  $\Delta P$ ). A system fault can be detected, if the error margin is smaller than the energy loss due to the system fault. For comparison 15% (solid line) and 30 % energy loss (dashed line) are marked.

Fig. 5 shows:

- For hourly values (left figure) the variation of expected errors is large. For high power production a significant amount of situations with error margins smaller than 15 % are

afternoon. The field test has revealed that shading at low sun elevations could be detected successfully within a few days. Considering only time of day did not result in a failure indication. The method is also capable to detect very minor shading in the early morning and late afternoon. Due to the definition of shading, shading e.g. in mid-afternoon will not be detected. Furthermore, the field test revealed that a wrong specified azimuth of a PV system results in an indication for shading. In the failure profiling, shading is defined as a significant energy loss at more than three hours a day. Therefore, shading over the day can be detected. Both routines add to each other.

General failure type	Failure
Constant energy loss	Degradation
	Soling
	Module defect
	String defect
Changing energy loss	Shading
	Grid outage
	High losses at low power
	Power limitation
	MPP tracking
	Hot inverter
	High temperature
Snow cover	Snow cover
Total blackout	Defect inverter
	Defect control devices

Other failures due to constant power loss could be detected by the footprint method very well in summer if the energy loss are larger than 20%. Power limitation is recognised very well at hours with high irradiation and low power production. The correct identification of failures and the required time by the footprint method is strongly dependent on the weather condition. The failure profiling has shown that it is difficult to distinguish the different failure types on the daily basis. Therefore, in the first step an unknown failure is detected, then the general failure type determined, and lastly, probabilities are assigned to the possible single failures.

#### 4. Conclusion

The automated failure detection as well as the identification depends strongly on the accuracy of the irradiance data which are used to calculate a comparison value. The technical description of a PV system has to be correct, otherwise a failure, which has not occurred, is falsely detected. This investigation “under laboratory conditions” has shown that all time scale are needed for a successful detection and identification of a malfunction. A minor energy loss of less than 15% can be detected using only satellite data with a coarse temporal and spatial resolution during the summertime examining the monthly power production. On the daily time scale under clear sky condition a failure with 15% energy loss can be recognised. Under broken cloud conditions the detection of a malfunction takes more time. The hourly values do not allow the detection of a system fault, but they are necessary for the identification of the most likely failure source.

Tab. 4 Detectable failures

The field test has shown that this conditions can be met. Usually an energy loss has been in the range of ~20% and larger when it has been detected successfully and the most likely failure source has been determined. Depending on the time of the year the needed period for the identification ranged between a few days up to three month.

#### References

- [1] A. Drews, A.C. de Keizer, H.G. Beyer, E. Lorenz, J. Betcke, W.G.J.H.M. van Sark, W. Heydenreich, E. Wiemken, S. Stettler, P. Toggweiler, S. Bofinger, M. Schneider, G. Heilscher, D. Heinemann, Monitoring and remote failure detection of grid-connected PV systems based on satellite observations, submitted to Solar Energy 03/2006.
- [2] A. Hammer, D. Heinemann, C. Hoyer, R. Kuhlemann, E. Lorenz, R.W. Mueller, H.G. Beyer, Solar resource assessment using remote sensing technologies. Remote Sensing of Environment, 86 (2003) 423.
- [3] E. Lorenz, Improved diffuse radiation model (PVSAT-2) Energy, Environment, and Sustainable Development Report, EU contract ENK5-CT-2002-00631, 2004.
- [4] J. Betcke, H.G. Beyer, Accuracy improvement of irradiation data by combining ground and satellite measurements, Proceedings of the EUROSUN2004 (2004) 764.